THE JOURNAL OF NAVIGATION (2002), **55**, 293–304. © The Royal Institute of Navigation
DOI: 10.1017/S0373463302001789 Printed in the United Kingdom

Ionospheric Correction for GPS Tracking of LEO Satellites

Oliver Montenbruck and Eberhard Gill

(*German Aerospace Center DLR*)

This paper describes an ionospheric correction technique for single frequency GPS measurements from satellites in low Earth orbit. The fractional total electron content (TEC) above the receiver altitude is obtained from global TEC maps of the International GPS Service network and an altitude dependent scale factor. By choosing a suitable effective height of the residual ionosphere, the resulting path delay for positive elevations is then computed from a thin layer approximation. The scale factor can be predicted from the assumption of a Chapman profile for the altitude variation of the electron density or adjusted as a free parameter in the processing of an extended set of single frequency measurements. The suitability of the proposed model is assessed by comparison with flight data from the Champ satellite that orbits the Earth at an altitude of 450 km. For the given test case, a 90% correction of the ionospheric error is achieved in a reduced dynamic orbit determination based on single frequency C/A-code measurements.

KEY WORDS

1. Space Tracking. 2. GPS.

1. INTRODUCTION. With the increased availability of flight-proven and affordable receivers for space applications, GPS has today evolved into a widely accepted tracking system for Low Earth Orbiting (LEO) satellites (Hart *et al.*, 1996; Bisnath & Langley, 1996; Gill *et al.*, 2000; Unwin *et al.*, 2000). Following the switch-off of intentional signal degradation (selective availability – S/A) of the GPS satellites in May 2000 (White House, 2000), even common L1 C/A-code receivers can now provide position and orbit information in the region of 1–10 m accuracy. In view of the public availability of precise GPS orbit and clock solutions (Beutler *et al.*, 1998), the achievable accuracy of single frequency measurements from low altitude spacecraft is thus mainly limited by ionospheric refraction effects. Depending on the altitude of the user spacecraft and the apparent elevation of the observed GPS satellites, the associated ionospheric signal delays may well amount to several tens of metres.

In this study, an ionospheric correction model is discussed, which makes use of global total electron content (TEC) maps from the International GPS Service (IGS) network. Assuming a Chapman profile to describe the altitude variation of the electron density, an estimate of the fractional TEC above the receiver altitude is derived. The ionospheric path delay for positive elevations is then obtained from a thin layer approximation with a suitably chosen effective height above the receiver. The performance of the proposed model is validated using flight data from the Champ mission. Champ orbits the Earth at an altitude of 450 km and carries a dual

frequency GPS receiver, which allows a direct measurement of the ionospheric range delay from P1 and P2 pseudo-ranges.

2. IONOSPHERIC CORRECTION MODEL. In accordance with common models for the ionospheric correction of terrestrial GPS measurements, a single layer approximation is proposed to describe the ionospheric path delay of spaceborne pseudo-range measurements. Given a satellite at altitude h_s above the surface of the Earth, we assume the residual ionosphere above the satellite to be concentrated in a single layer at altitude $h_{IP} > h_S$. A signal received by the spacecraft at location $\boldsymbol{r}_S$ with a positive elevation E_S traverses the spherical ionospheric layer once at the ionospheric point (IP) with elevation $E_{IP} \geqslant E$ (See Figure 1). Denoting the total

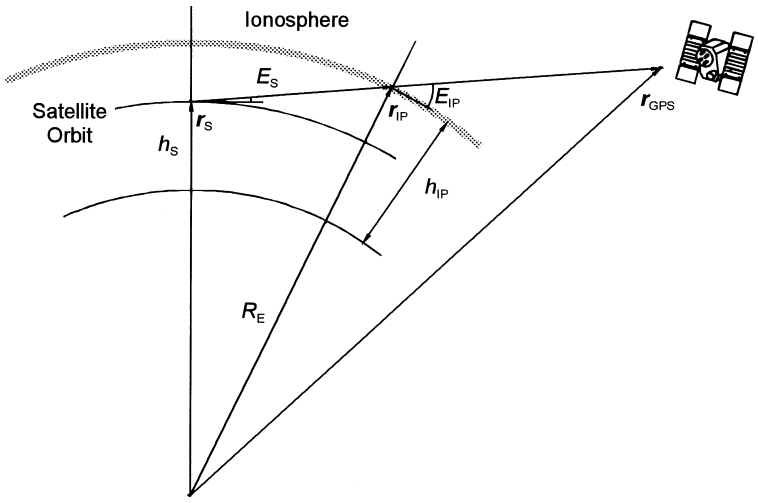

Figure 1. Geometry of thin layer ionosphere correction model for satellite orbits.

vertical electron content at location $\boldsymbol{r}$ as the integral of the electron density d_e along the local vertical from radius r to infinity, the ionospheric path delay is directly proportional to the TEC value at the ionospheric point $\boldsymbol{r}_{IP}$

$$\mathrm{TEC}(\boldsymbol{r}) = \int_r^\infty d_e(s \cdot \boldsymbol{r}/r)\,\mathrm{d}s. \tag{1}$$

Pseudo-range measurements taken at the L1 frequency experience a group delay

$$\Delta\rho_{L1} = \frac{1}{\sin(E_{IP})}\frac{40{\cdot}3\ \mathrm{m}^3\ s^{-2}}{f_{L1}^2}\mathrm{TEC}(\boldsymbol{r}_{IP}) = \frac{0{\cdot}162\ \mathrm{m}}{\sin(E_{IP})}\frac{\mathrm{TEC}(\boldsymbol{r}_{IP})}{10^{-16}\ \mathrm{m}^{-2}}, \tag{2}$$

where the mapping function

$$M(E_{IP}) = \frac{1}{\sin(E_{IP})} = \{1 - [\cos(E_S) \cdot r_S/r_{IP}]^2\}^{-1/2} \tag{3}$$

accounts for the increase of the path length in the ionosphere with decreasing elevation (cf. Hofmann-Wellenhoff *et al.*, 1997).

https://doi.org/10.1017/S0373463302001789 Published online by Cambridge University Press

Given the geocentric positions of the GPS satellite ($\boldsymbol{r}_{\mathrm{GPS}}$) and the user satellite ($\boldsymbol{r}_{\mathrm{S}}$), the position of the ionospheric point is obtained from the intersection of the line-of-sight vector with a sphere of radius $r_{\mathrm{IP}} = R_{\mathrm{E}} + h_{\mathrm{IP}}$ around the centre of the Earth. This yields the condition

$$|\boldsymbol{r}_{\mathrm{S}} + \mu(\boldsymbol{r}_{\mathrm{GPS}} - \boldsymbol{r}_{\mathrm{S}})| = r_{\mathrm{IP}} \tag{4}$$

for the fractional distance μ of the ionospheric point from the observer along the connecting line to the GPS satellite. By solving the resulting quadratic equation, one obtains the expression:

$$\boldsymbol{r}_{\mathrm{IP}} = \boldsymbol{r}_{\mathrm{S}} + [\sqrt{x^2 + (r_{\mathrm{IP}}^2 - r_{\mathrm{S}}^2)/d^2} - x] \cdot \boldsymbol{d}, \tag{5}$$

for the location of ionospheric point, where:

$$\boldsymbol{d} = \boldsymbol{r}_{\mathrm{GPS}} - \boldsymbol{r}_{\mathrm{S}}, \tag{6}$$

denotes the line-of-sight vector and:

$$x = (\boldsymbol{d}^T \boldsymbol{r}_{\mathrm{S}})/d^2, \tag{7}$$

is an auxiliary quantity.

The above relations describe the geometric variation of the ionospheric path delay for different locations of the observer and the GPS satellite under the provision that the effective altitude and the total electron content of the residual ionosphere are known. While the geographical variation of the total electron content is readily accessible today from ground-based observations of GPS satellites, the restitution of the vertical stratification of the ionosphere is severely limited by the restricted observation geometry (Kleusberg, 1998). Reference to theoretical models like the International Reference Ionosphere IRI95 (Bilitza *et al.*, 1995) must therefore be made to obtain information on the altitude variation of the ionospheric electron density. Its use is complicated, however, by the fact that the predicted density values do not converge to zero within the limited altitude range of the model (1000 km). A direct application of the model thus introduces a considerable uncertainty in the prediction of the effective altitude and the total electron content of the residual ionosphere. As a remedy, we have therefore decided to approximate the IRI95 density values by a Chapman profile:

$$d_{\mathrm{e}}(h) = d_0 \cdot \exp(1 - z - \exp(-z)), \quad z = (h - h_0)/H, \tag{8}$$

with suitably adjusted inflection point altitude h_0 and scale height H. Let the effective altitude of the residual ionosphere above altitude h_{S} be defined as the 50 percentile altitude, then:

$$\int_{h_{\mathrm{S}}}^{h_{\mathrm{IP}}} \exp(1 - z - \exp(-z))\,\mathrm{d}h = \tfrac{1}{2}\int_{h_{\mathrm{S}}}^{\infty} \exp(1 - z - \exp(-z))\,\mathrm{d}h. \tag{9}$$

Making use of the indefinite integral:

$$\int \exp(1 - z - \exp(-z))\,\mathrm{d}z = \exp(1 - \exp(-z)), \tag{10}$$

one finally obtains the condition:

$$\exp(1 - \exp(-z_{\mathrm{IP}})) = \tfrac{1}{2}(e + \exp(1 - \exp(-z_{\mathrm{S}}))), \tag{11}$$

https://doi.org/10.1017/S0373463302001789 Published online by Cambridge University Press

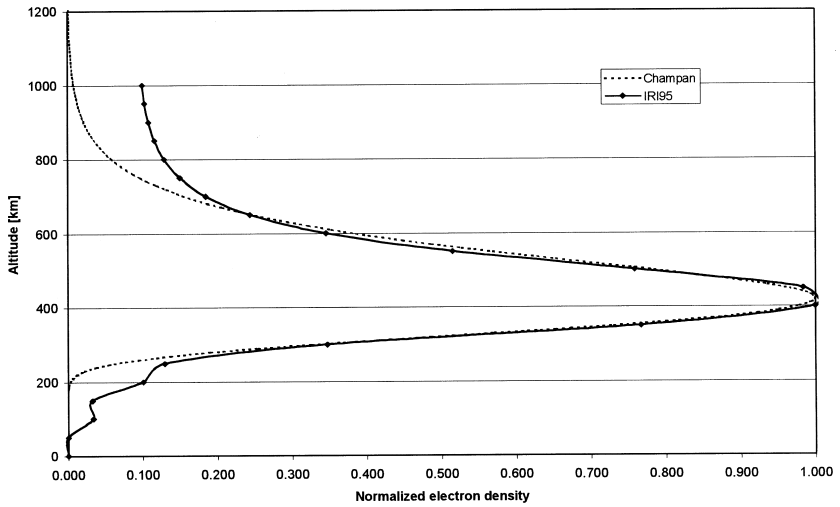

Figure 2. Normalized electron density profile near the global TEC maximum on 7 August 2000 ($\varphi = 0°$, $l = -140°$, $t = 1{:}00$ UTC) from the International Reference Ionosphere IRI95. The density variation is best represented by a Chapman profile with scale height $H = 100$ km and inflection point height $h_0 = 420$ km.

which can readily be solved for z_{IP} and thus h_{IP}. Likewise, one may relate the total electron content $\mathrm{TEC}(\lambda_{\mathrm{IP}}, \varphi_{\mathrm{IP}}, h_{\mathrm{IP}})$ of the ionosphere above altitude h_{IP} to the total electron content above ground at geographical coordinates $(\lambda_{\mathrm{IP}}, \varphi_{\mathrm{IP}})$ by the scaling factor

$$\alpha = \frac{\mathrm{TEC}(\lambda_{\mathrm{IP}}, \varphi_{\mathrm{IP}}, h_{\mathrm{IP}})}{\mathrm{TEC}(\lambda_{\mathrm{IP}}, \varphi_{\mathrm{IP}}, 0)} = \frac{\int_{h_{\mathrm{IP}}}^{\infty} \exp(1 - z - \exp(-z))\,\mathrm{d}h}{\int_{0}^{\infty} \exp(1 - z - \exp(-z))\,\mathrm{d}h}$$

$$= \frac{e - \exp(1 - \exp(-z_{\mathrm{IP}}))}{e - \exp(1 - \exp(h_0/H))}. \tag{12}$$

A sample Chapman profile with inflection point height $h_0 = 420$ km and scale height $H = 100$ km is illustrated in Figure 2. It provides a close approximation of the IRI95 density values on 7 August 2000 near the location of the global TEC maximum.

Although the vertical electron density profile varies with the angular separation of the ionospheric point from the sub-solar point, we may neglect this variation in a first approximation and assume α to be constant along the satellite orbit. Making use of global surface TEC maps as provided by the IGS or the Klobuchar model (1996), the ionospheric path delay for a given pseudo-range measurement can ultimately be predicted as

$$\Delta\rho_{\mathrm{L1}}^{\mathrm{pred}} = \alpha \frac{0{\cdot}162\ \mathrm{m}}{\sin(E_{\mathrm{IP}})} \frac{\mathrm{TEC}(\lambda_{\mathrm{IP}}, \varphi_{\mathrm{IP}}, 0)}{10^{-16}\ \mathrm{m}^{-2}}, \tag{13}$$

where the geographical coordinates of the ionospheric point and the elevation of the line-of-sight vector depend on the positions of the user satellite and the GPS satellite as well as the adopted reference height h_{IP} of the residual ionosphere.

https://doi.org/10.1017/S0373463302001789 Published online by Cambridge University Press

3. CHAMP DATA SET. The Champ micro satellite, which was launched on 15 July 2000, and orbits the Earth at an altitude of 450 km, is the first of a series of scientific and remote sensing satellites equipped with a geodetic quality GPS receiver developed by the Jet Propulsion Laboratory. Key mission goals comprise the derivation of accurate and self-contained gravity field models as well as limb sounding of the Earth atmosphere (Reigber *et al.*, 1996). The Blackjack receiver carried onboard the Champ satellite is a cross-correlation GPS receiver providing code and phase measurements on both the L1 and L2 frequencies (Kuang *et al.*, 2001). It is a follow-on of the Turbo-Rogue receiver previously flown on, for example, the Microlab-1 mission as part of the GPS/MET project (Bisnath & Langley, 1996).

A first set of GPS measurements and an associated reference trajectory was released in early December 2000 by the Champ project (Champ, 2000b). The data, collected on 7 August 2000, covers 24 hours of measurements at a rate of one value per 10 seconds. For the ionosphere free linear combinations of L1 and L2 P-code pseudo-ranges, an rms error of 1·3 m has been determined by Kuang *et al.* (2001).

Within this study, use has been made of L1 C/A-code pseudo-ranges as well as L1/L2 P-code pseudo-ranges. The dual frequency data provide direct measurements of ionospheric refraction effects for calibration and verification of the proposed correction model. By contrast, the C/A-code measurements serve as an independent data set, which is considered to be representative of common single frequency receivers. Together with a rapid science orbit, which provides a precise reference trajectory for the concerned time interval, the C/A-code data were used for the analysis of achievable single-point positioning solutions.

4. ANALYSIS AND RESULTS.

4.1. *Comparison with Observed Ionospheric Path Delays.* Since the ionospheric path delay $\Delta\rho$ is inversely proportional to the signal frequency f, the difference of the L1 and L2 pseudo-ranges ρ_{L1} and ρ_{L2} yields – in the absence of other errors – a direct measure of the L1 path delay:

$$\Delta\rho_{L1}^{meas} = \frac{f_2^2}{f_1^2 - f_2^2} \cdot (\rho_{L2} - \rho_{L1}) = 1{\cdot}546 \cdot (\rho_{L2} - \rho_{L1}). \tag{14}$$

These observations may be compared against the values predicted by (13) with suitable values for the reference height and the fractional TEC above the Champ orbit. Making use of Chapman profiles adjusted to the IRI95 density values for 7 August 2000, an effective altitude of 540 km (570 km) and a 50 % (40 %) fraction of the TEC content measured at ground are expected for the residual ionosphere above a satellite at altitude 450 km near the global TEC maximum (minimum). Accurate TEC values for the day of interest (Figure 3) have furthermore been made available by the Center of Orbit Determination in Europe (CODE) in Berne (AIUB, 2000).

To assess the quality of the proposed model, the measured ionospheric path delays have been compared against predicted values assuming a reference height $h_0 = 550$ km and a fractional TEC of $\alpha = 1$. In view of a notable scatter of the measurements collected at low elevations, the comparison has been restricted to observations with elevations of more than 10° and bad data points have been removed by checking the pseudo-range residuals with respect to the reference orbit.

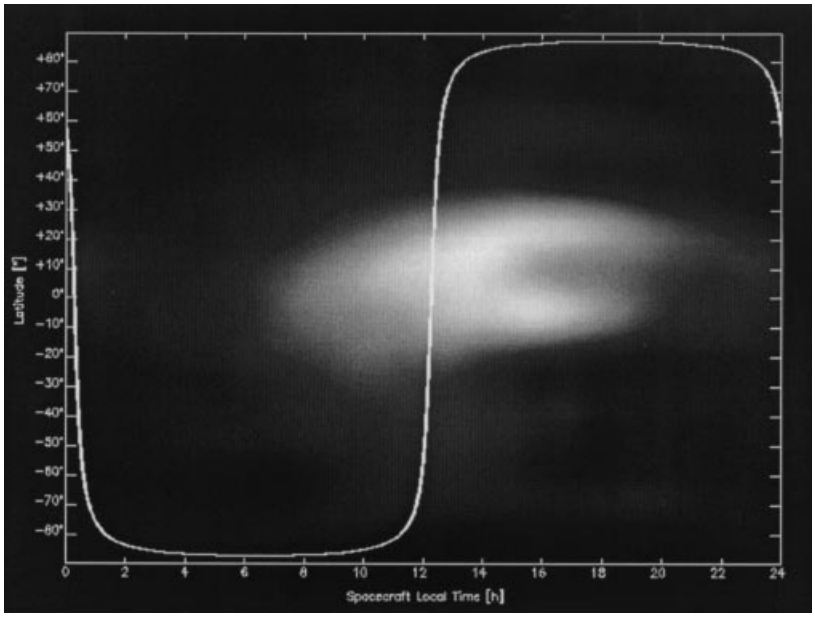

Figure 3. Global TEC map (AIUB) for 7 August 2000 – 1200 hours, as a function of geographic latitude and mean solar local time ($T = \mathrm{UTC} + \lambda$). The solid line indicates the ground track of the Champ satellite orbit, which maintains an essentially constant orientation in the given reference frame. TEC values range from 0 (black) to 100 TEC units (white). Along the Champ orbit, maximum TEC values of about 80-90 TECU are encountered near the ascending node crossing, while a secondary maximum of 20-40 TECU is located near the descending node.

The results shown in Figure 4 have a good overall correlation, which is best represented by the linear relation:

$$[1{\cdot}546 \cdot (\rho_{L2} - \rho_{L1})] = 3{\cdot}8\ \mathrm{m} + 0{\cdot}32 \cdot \left[\frac{0{\cdot}162\ \mathrm{m}}{\sin(E_{IP})} \frac{\mathrm{TEC}(\lambda_{IP}, \varphi_{IP}, 0)}{10^{-16}\ \mathrm{m}^{-2}} \right]. \qquad (15)$$

The calibrated offset of 3·8 m indicates a differential code bias (DCB) of 2·4 m or, equivalently, 8 ns between the L2 and L1 code phase measurements of the Champ Blackjack receiver. This value is in good accord with representative DCB values of dual frequency receivers as determined in the analysis of global observations sets from the IGS or NSTB networks (Hansen, 1998). While, in principle, it would also be necessary to account for the DCB of the GPS satellites themselves, the corresponding values are generally much smaller than the receiver DCBs (1 ns to 2 ns), and have therefore been ignored in the current analysis.

The linear regression (15) predicts individual ionospheric path delay with an r.m.s. accuracy of 3 m and provides an empirical calibration $\alpha^{\mathrm{calib}} = 0{\cdot}32$ of the fractional electron content of the ionosphere above the Champ orbit. Obviously the adjusted value is substantially smaller than the value $\alpha^{\mathrm{pred}} = 0{\cdot}40\,..\,0{\cdot}50$ expected from the IRI95 model, which indicates a practical limitation of a purely model-based ionospheric correction. One may, however, consider α as a free scaling parameter and adjust its value in a single point positioning (using suitable *a priori* constraints) or a dynamic orbit determination. Before following this approach, however, we first assess

https://doi.org/10.1017/S0373463302001789 Published online by Cambridge University Press

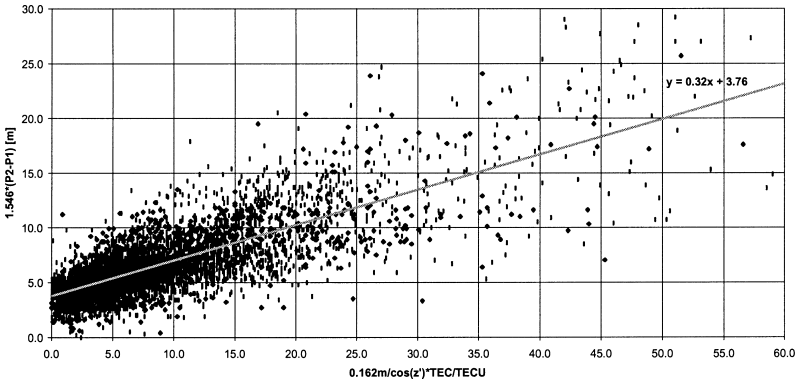

Figure 4. Calibration of the differential code bias and the fractional TEC of the ionosphere above the Champ orbit on 7 August 2000 from the correlation of observed ionospheric range delays with computed values (see text for further explanation).

the achievable benefit of the calibrated correction model in a C/A-code single point positioning.

4.2. *C/A-Code Single Point Positioning*. Making use of precise GPS orbits and clock solutions provided by the IGS, kinematic point positions for the Champ satellite have been obtained from various combinations of raw pseudo-ranges and ionospheric corrections. Modelled pseudo-ranges have been corrected for the GPS satellite clock offset, the relativistic GPS satellite clock offset and the GPS satellite antenna offset. For each time step, the available pseudo-ranges were then used to estimate the WGS84 coordinates of Champ's main POD antenna and the Blackjack receiver clock offset in an unconstrained least-squares adjustment. Finally, the obtained antenna coordinates were transformed to the centre-of-gravity of the spacecraft assuming a nominal alignment of the s/c axes with the local nadir, cross-track and flight direction and antenna offsets given in Champ (2000a). The data set used in the analysis was sampled at 60 s intervals and covers 24 hours starting on 7 August 2000, 0 hrs GPS time. Reference positions were obtained from the GFZ rapid science orbit for the same date.

While typical pseudo-range errors of the Blackjack receiver amount to roughly one metre (Kuang *et al*., 2001), the Champ test data set used in the analysis exhibits frequent outliers on the order of 10 m to 100 km. A thorough screening of individual measurements is therefore required to obtain meaningful single point solutions. Following a careful inspection of individual pseudo-range residuals, all measurements performed below an elevation limit of 10° were discarded. The complete data point (comprising all pseudo-ranges obtained at the same epoch) was furthermore ignored, if the root-mean-square of the pseudo-range residuals after the adjustment exceeded a threshold of 2·5 m or if the position-dilution-of-precision (PDOP) was larger than 10 (implying an unfavorable observation geometry). In this way, it was ensured that no erroneous measurements affected the computed single point position solutions and the envisaged assessment of the ionospheric correction model.

The resulting mean and r.m.s. position errors as well as the mean and r.m.s. errors along the radial, east and north direction are summarized in Table 1. Case 1 is based on L1 band P-code measurements with ionospheric corrections derived from the L2/L1 P-code differences. It illustrates the achievable position accuracy of about 2 m

https://doi.org/10.1017/S0373463302001789 Published online by Cambridge University Press

Table 1. Single point positioning accuracy for Champ satellite on 7 August 2000, using 24 hours of pseudo-range measurements sampled at 60 s intervals. Reference positions are based on the GFZ rapid science orbit for the same day. Outliers have been removed by requiring a minimum elevation of 10°, a PDOP of less than 10 and a maximum post-fit pseudo-range r.m.s. of 2·5 m at each time step. In accordance with the conventional RINEX notation, the data type keys C1, P1 and P2 designate C/A-code pseudo-ranges, L1 P-code pseudo-ranges and L2 P-code pseudo-ranges, respectively. Mean and r.m.s. values shown in metres.

Case	Data type	Ionospheric Correction	Position		Radial		East		North	
			mean	r.m.s.	mean	r.m.s.	mean	r.m.s.	mean	r.m.s.
1	P1	P2-P1 difference	3·22	2·64	+0·17	3·72	+0·01	0·92	+0·04	1·60
2	C1	P2-P1 difference	2·89	2·61	+0·21	3·44	−0·06	0·84	+0·03	1·61
3a	C1	TEC map (CODE), $\alpha = 0{\cdot}32$, $h_0 = 550$ km	3·20	2·28	+0·27	3·49	−0·20	0·92	−0·05	1·50
3b	C1	$\alpha = 0{\cdot}26$, $h_0 = 550$ km	3·31	2·40	+0·95	3·54	−0·20	0·93	−0·03	1·54
4	C1	None	4·58	3·13	+3·58	3·84	−0·12	0·96	−0·04	1·51

in the horizontal plane and 4 m in the radial direction, which is likewise obtained, if C/A-code pseudo-ranges are processed in the same manner (Case 2).

The achievable accuracy of the proposed ionospheric correction model is illustrated in Case 3a. Here, ionospheric path delays have been predicted from two-dimensional TEC maps obtained from CODE and used to correct the C/A-code pseudo-ranges. The computation was performed with an assumed value of $h_0 = 550$ km for the effective height of the residual ionosphere and the best-fit value $\alpha^{\mathrm{calib}} = 0{\cdot}32$ was adopted for the fractional TEC above the Champ orbit. The accuracies of the obtained point solution differ only slightly from Cases 1 and 2, which provides a preliminary justification of the model and its inherent assumptions and simplifications. We note, however, that use of the modelled ionospheric corrections introduces a small offset of 0·20 m in the East/West component. Apparently, this offset is caused by an asymmetric orientation of the Champ orbit with respect to the ionospheric bulge and a non-uniform quality of the model for different locations.

On the other hand, application of the predicted corrections to the single frequency C/A-code measurements evidently offers a notable accuracy gain over the use of uncorrected pseudo-ranges. As illustrated by a comparison of Cases 3a and 4, the ionospheric correction essentially removes a systematic radial bias of 3·7 m, which is otherwise present in the C/A-code position solution.

4.3. *C/A-code Single Point Positioning with Fractional TEC Calibration.* While the analysis performed above demonstrates the overall validity of the proposed ionospheric correction model for low Earth satellites, it is unrealistic in the sense that the optimum value of α has been adjusted from dual frequency measurements. In practice, no such calibration is available when using a simple L1 C/A-code receiver, and α has thus to be obtained from other sources. Since independent predictions of the fractional electron content above the satellite orbit based on the IRI95 model have already been shown to yield unsatisfactory results, the calibration of α from single frequency C/A-code measurements has therefore been studied.

To this end, we note that the functional dependence of the ionospheric range

https://doi.org/10.1017/S0373463302001789 Published online by Cambridge University Press

correction on the relative location of the user satellite and the GPS satellite is adequately described by the thin layer model (13). The fractional electron content α thus represents a single common scaling parameter for all observations that can be adjusted to minimize the overall pseudo-range residuals in a least squares sense. To avoid the simultaneous adjustment of position and clock values for all measurement times and the associated high-dimensional system of normal equations, a sequential batch filter has been chosen for the practical implementation. At each time step i, a five-dimensional state vector:

$$\boldsymbol{x}_i = \begin{pmatrix} \boldsymbol{r}_i \\ c\delta t_i \\ \alpha_i \end{pmatrix}, \tag{16}$$

is adjusted from the pseudo-ranges collected at this time, where $\boldsymbol{r}_i$ is the instantaneous position of the user satellite, $c\delta t_i$ is the receiver clock offset (expressed in units of length) and α is the TEC fraction of the upper ionosphere. The resulting least squares problems are non-linear and require multiple iterations at each time step to achieve convergence. Information between consecutive time steps is passed by adopting the estimated value of α and its associated standard deviation $\sigma(\alpha)$ at a given step as *a priori* values for the subsequent step. *A priori* values for position and clock error, in contrast, are taken from a reference trajectory and the corresponding *a priori* standard deviations are chosen large enough (1 km) to allow an essentially unconstrained adjustment of these components in each step.

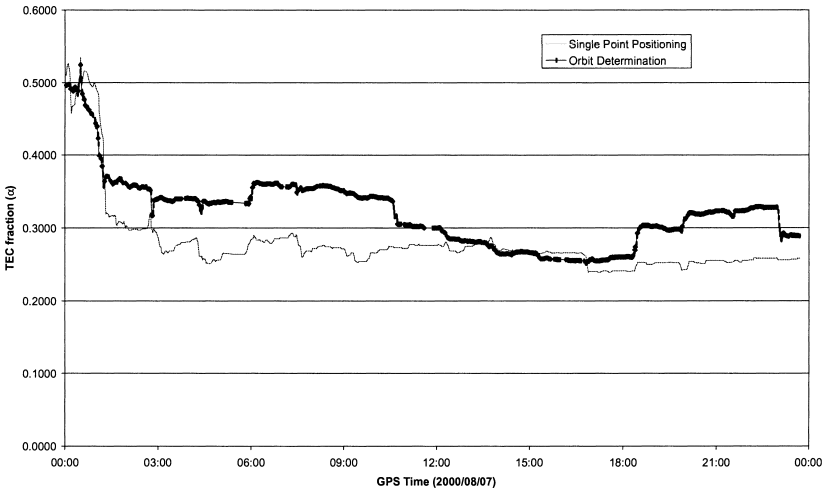

Figure 5. Sequential filtering of the ionospheric scale parameter α from single frequency C/A-code pseudo-ranges of the Champ satellite on 7 August 2000.

Starting from assumed initial values of $\alpha = 0{\cdot}5$ and $\sigma(\alpha) = 0{\cdot}1$, the filter converges within one revolution (1·5 hours), during which the standard deviation decreases to roughly 50 % of the *a priori* value (Figure 5). Thereafter, the estimated TEC fraction α varies between 0·24 and 0·30 and achieves a final value of $\alpha^{\text{est}} = 0{\cdot}26$ after processing of the complete data arc. This value is notably less than the result obtained from

https://doi.org/10.1017/S0373463302001789 Published online by Cambridge University Press

Table 2. Accuracy of reduced dynamic orbit determination for Champ satellite on 7 August 2000, using 24 hours of pseudo-range measurements sampled at 60 s intervals. Reference positions are based on the GFZ rapid science orbit for the same day. Outliers have been removed by requiring a minimum elevation of 10° and a maximum post-fit pseudo-range r.m.s. of 2·5 m at each time step. Mean and r.m.s. values shown in metres.

Case	Data type	Ionospheric Correction	Position		Radial		East		North	
			mean	r.m.s.	mean	r.m.s.	mean	r.m.s.	mean	r.m.s.
1	P1	P2-P1 difference	1·06	0·56	+0·05	0·74	+0·04	0·65	+0·02	0·67
2	C1	P2-P1 difference	1·05	0·55	+0·18	0·69	−0·02	0·67	−0·00	0·67
3a	C1	TEC map (CODE), $\alpha = 0{\cdot}32$, $h_0 = 550$ km	1·78	0·88	+0·15	1·32	−0·28	0.·87	+0·05	1·17
3b	C1	α estimated, $\alpha_0 = 0{\cdot}30$	1·77	0·92	+0·35	1·31	−0·28	0·86	+0·04	1·15
4	C1	None	4·00	1·36	+3·58	1·46	−0·33	1·12	+0·01	1·24

P2-P1 observations in the previous section, but is nevertheless statistically well determined with a final standard deviation of $\sigma(\alpha) = 0{\cdot}016$. Indeed, the overall r.m.s. of the pseudo-range residuals is found to be marginally smaller for an assumed value of $\alpha = 0{\cdot}26$ than for the calibration result $\alpha = 0{\cdot}32$. As a consequence, the resulting position estimates exhibit a systematic radial offset of about 1 m (cf. Table 1, Case 3b). Taking this offset as a quality measure of the proposed ionospheric correction model, the applied corrections account for merely 73 % of the total effect on the computed single point position solutions. This is notably worse than might have been expected from the results of the previous section. As will be shown next, however, improved estimates for the ionospheric scaling parameter can be obtained in a dynamic orbit determination. It is, therefore, suspected that the slightly discouraging single point positioning results are due to the increased sensitivity of the radial position component to systematic errors in the measurements and/or the measurement processing.

4.4. *C/A-code Orbit Determination Results.* Complementary to the kinematic single point positioning described above, the Champ C/A-code pseudo-ranges have been processed in a reduced dynamic orbit determination. The deterministic part of the applied force model comprises the Earth's gravity field up to degree and order 50, the luni-solar gravitation, the solar radiation pressure and atmospheric drag. Since neither the selected JGM-3 gravity field model (Tapley *et al.*, 1996) nor the simplifying Harries-Priester drag model (Long *et al.*, 1989) provide a sufficiently accurate representation of the actual perturbations affecting a satellite in a 450 km altitude orbit, empirical accelerations in the radial, along-track and cross-track directions have been considered in the analysis. The Kalman filter parameters comprise the 6-dimensional state vector $(\boldsymbol{r}, \boldsymbol{v})$ of the satellite, the GPS receiver clock error $(c\delta t)$, the 3-dimensional vector of empirical accelerations $(\boldsymbol{a}_{\mathrm{emp}})$, and, optionally, the ionospheric scaling parameter (α). For each parameter, appropriate diagonal elements of the process noise matrix have been chosen such as to obtain optimal filter results. In view of evident correlations with the adjusted accelerations, the drag and solar radiation pressure coefficient have been held fixed at suitable *a*

https://doi.org/10.1017/S0373463302001789 Published online by Cambridge University Press

priori values. Again, the GFZ rapid science orbit served as reference for the resulting position estimates.

As shown in Table 2, the errors of the filtered trajectory exhibit a notably smaller scatter than the single point solutions. This is particularly true for the radial component, which otherwise exhibits an unfavorable geometric dilution of precision and benefits most from the constraints introduced by the dynamical model. Using observed ionospheric corrections from dual frequency measurements, resulting r.m.s. errors of about 0·7 m are achieved in each axis (Case 1 & 2). Slightly larger errors of 0·9 m to 1·3 m as well as a small bias in East/West direction may be observed for the ionospheric correction model, when using the calibrated TEC fraction of $\alpha = 0{\cdot}32$ (Case 3a).

Upon adjusting the ionospheric scale parameter α along with the other filter parameters, it takes about 1 revolution (1·5 hours) to achieve convergence from initial conditions of $\alpha_0 = 0{\cdot}5$ with standard deviation $\sigma(\alpha_0) = 0{\cdot}1$ (Figure 5). Thereafter the estimate varies over time between a minimum of $\alpha = 0{\cdot}26$ and a maximum of $\alpha = 0{\cdot}37$. Major jumps in the estimated value may be observed once per orbit coinciding with TEC maxima at the crossing of the ionospheric bulge. Compared to the single point positioning, the estimated scaling parameter is generally higher, which reflects a better performance of the ionospheric correction model. As shown in Case 3b, the adjustment of the TEC scaling parameter as part of the dynamical filtering (using a starting value of $\alpha_0 = 0{\cdot}3$) yields a trajectory with a mean radial offset of 0·34 m. Considering that the use of uncorrected C/A-code measurements results in a 3·6 m offset (Case 4), the model thus accounts for roughly 90 % of the total ionospheric effects.

5. SUMMARY AND CONCLUSIONS. In combination with global, 2-dimensional TEC maps, the thin-layer approximation of the ionosphere above a low Earth satellite provides a suitable model for the ionospheric correction of single frequency pseudo-range measurements from space-borne GPS receivers. Apart from the effective height of the residual ionosphere, which may be derived from existing ionospheric models with adequate accuracy, the model involves an altitude-dependent scaling factor for the fraction of the ground-based total electron content. Using a calibrated value of the TEC scaling factor, the predicted corrections of individual pseudo-ranges match the dual frequency correction with an r.m.s. error of 3 m for a one-day sample of GPS measurements from the Champ satellite. At the same time, single point positioning results derived from the corrected measurements are essentially bias free, whereas the use of uncorrected L1 C/A-code pseudo-ranges results in a radial offset of roughly 4 m.

For practical applications, the accuracy of the model is limited by the capability to adjust the TEC scaling factor from an extended set of single frequency observations or to predict its value from independent ionospheric models. Restricting oneself to C/A-code pseudo-ranges, optimum results have been obtained in a dynamic orbit determination, in which the fractional TEC above the satellite orbit is estimated along with other state parameters. Here a 90 % correction of the total ionospheric effects on the filtered trajectory has been demonstrated for the sample Champ data set. For a corresponding single point positioning, the reduced position dilution of precision results in an inferior estimate of the TEC scaling parameter and the achieved ionospheric correction accounts for only 73 % of the total effect on average.

ACKNOWLEDGMENTS

The present study makes extensive use of Blackjack GPS receiver measurements that have been made available by GFZ, Potsdam, and JPL, Pasadena. Ionospheric TEC data employed in the analysis have, furthermore, been provided by CODE, Berne, as part of the IGS. The authors are grateful to M. Rothacher for technical discussions and valuable comments on the subject of GPS-based positioning and orbit determination.

REFERENCES

AIUB (2000). Global ionosphere maps (GIMs). *Produced by CODE*. http://www.aiub.unibe.ch/ionosphere.html.

Beutler, G., Rothacher, M., Springer, T., Kouba, J. and Neilan, R. E. (1998). International GPS Service (IGS): an interdisciplinary service in support of Earth sciences. *32nd COSPAR Scientific Assembly*, Nagoya, Japan, July 12 to 19 (1998).

Bilitza, D., Koblinsky, C., Beckley, B., Zia, S. and Williamson, R. (1995). Using IRI for the computation of ionospheric corrections for altimeter data analysis. *Adv. Space. Res.* vol. **15/2**, 113–119.

Bisnath, S. B. and Langley, R. B. (1996). Assessment of the GPS/MET TurboStar GPS receiver for orbit determination of a future CSA micro/small-satellite mission. *Dept. of Geodesy and Geomatics Engineering*, Univ. New Brunswick, Contract No. 9F011-5-0651/001/XSD.

Champ (2000a). Reference systems, transformations and standards. *GFZ Postdam*; Dec. 5.

Champ (2000b). *Champ Newsletter No. 2*; http://op.gfz-potsdam.de/champ; Dec 8.

Gill, E., Montenbruck, O. and Brieß, K. (2000). GPS-based autonomous navigation for the BIRD satellite. *15th International Symposium on Spaceflight Dynamics*, 26–30 June 2000; Biarritz.

Hansen, A. J. (1998). Real-time ionospheric tomography using terrestrial GPS sensors. *ION GPS-98, Paper A3-5*, Sept. 15–18, Nashville, Tennessee.

Hart, R. C., Gramling, C. J., Deutschmann, J. K., Long, A. C., Oza, D. H. and Steger, W. L. (1996). Autonomous navigation initiatives at the NASA GSFC Flight Dynamics Division. *96-c-23; Proceedings of the 11th IAS (International Astrodynamics Symposium)*, May 1996 Gifu, Japan, pp. 125–130.

Hofmann-Wellenhof, B., Lichtenegger, H. and Collins, J. (1997). *Global Positioning System Theory and Applications*. Springer-Verlag Wien, New York, 4th ed.

Kleusberg, A. (1998). Atmospheric models from GPS. *GPS for Geodesy*; Teunissen, P. J. G. and Kleusberg, A., Springer Verlag, Heidelberg, 2nd ed.

Klobuchar, J. A. (1996). Ionospheric effects on GPS. *Global Positioning System: Theory and Applications*, Chapter 12, Parkinson, B. W. and Spilker, J. J. Jr., AIAA, Washington.

Kuang, D., Bar-Sever, Y., Bertiger, W., Desai, S., Haines, B., Meehan, T. and Romans, L. (2001). Precise orbit determination for CHAMP using GPS data from BlackJack receiver. *ION National Technical Meeting*, Paper E1-5, January 22–24, Long Beach, California.

Long, A. C., Cappellari, J. O., Velez, C. E. and Fuchs, A. J. (1989). *Mathematical Theory of the Goddard Trajectory Determination System*; Goddard Space Flight Center; FDD/552-89/001; Greenbelt, Maryland.

Reigber, Ch., Bock, R., Förste, Ch., Grunwaldt, L., Jakowski, N., Lühr, H., Schwintzer, P. and Tilgner, C. (1996). *CHAMP Phase B – Executive Summary*; Scientific Technical Report STR96/13, GeoForschungsZentrum Potsdam.

Tapley, B. D., Watkins, M. M., Ries, J. C., Davis, G. W., Eanes, R. J., Poole, S. R., Rim, H. J., Schutz, B. E., Shum, C. K., Nerem, R. S., Lerch, F. J., Marshall, J. A., Klosko, S. M., Pavlis, N. K. and Williamson, R. G. (1996). The joint gravity model 3. *Journal of Geophysical Research* **101**, 28029–28049.

Unwin, M. J., Oldfield, M. K. and Purivigraipong, S. (2000). Orbital demonstration of a new space GPS receiver for orbit and attitude determination. *Int. Workshop on Aerospace Apps. of GPS*; 31 Jan.–2 Feb. 2000, Breckenridge, Colorado.

White House (2000). Statement by the President regarding the United States decision to stop degrading Global Positioning System accuracy. http://www.whitehouse.gov/library/PressPreleases.cgi; May 1st. *Office of the Press Secretary*.